Bioinorganics and Biocatalysis
https://www.sciltp.com/journals/bb

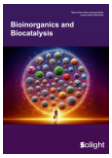

Article

α-Synuclein and Dopamine Metabolites DOPAL and DOPAC: A Pathway to New Synthetic Neuromelanin Models

Andrea Capucciati [1,2], Michela Sturini [1], Stefania Nicolis [1], Fabio A. Zucca [2], Marco Bisaglia [3], Giulia Favetta [3], Marco Bortolus [4], Luigi Zecca [2,5], Gianni Pezzoli [5], Luigi Casella [1] and Enrico Monzani [1,*]

[1] Department of Chemistry, University of Pavia, Via Taramelli 12, 27100 Pavia, Italy
[2] Institute of Biomedical Technologies, National Research Council of Italy, Via Cervi 93, 20054 Milan, Italy
[3] Department of Biology, University of Padova, Via Ugo Bassi 58/B, 35128 Padova, Italy
[4] Department of Chemical Sciences, University of Padova, Via Marzolo 1, 35131 Padova, Italy
[5] Pezzoli Foundation for Parkinson Disease, 20125 Milan, Italy
* Correspondence: enrico.monzani@unipv.it

How To Cite: Capucciati, A.; Sturini, M.; Nicolis, S.; et al. α-Synuclein and Dopamine Metabolites DOPAL and DOPAC: A Pathway to New Synthetic Neuromelanin Models. *Bioinorganics and Biocatalysis* **2025**, *1*(1), 2.

Received: 28 March 2025
Revised: 30 April 2025
Accepted: 6 May 2025
Published: 9 May 2025

Abstract: Melanin-protein-Fe conjugates serving as new synthetic analogues of brain neuromelanin were prepared by oxidative oligomerization of dopamine (DA) and its metabolites, 3,4-dihydroxyphenyl acetaldehyde (DOPAL) and 3,4-dihydroxyphenylacetic acid (DOPAC) in the presence of α-synuclein (αSyn), L-cysteine, and iron salts. The initial reaction of cysteine with the quinone derivatives of the catechols yields the corresponding cysteinyl-catechols which under iron promoted oxidative conditions convert to cysteinyl-quinones that undergo nucleophilic addition by the side chain of the protein lysines and tyrosines. In the case of dopamine, this reaction is in competition with internal cyclization by the amino group to generate melanochrome so that α-synuclein was found partially unmodified and non-covalently bound to the melanin moiety. For DOPAL and DOPAC the functional groups on the catechol side chains can further stabilize the melanin-protein conjugates through condensation or charge interaction with the several lysines present in αSyn. The presence of cysteine in the melanin component allows to classify the resulting conjugates as pheomelanin-αSyn-Fe derivatives of DA, DOPAL and DOPAC. The iron ions acting as catalysts are initially bound to the catechol groups and remain entrapped into the melanin moieties mostly associated in clusters, with less than 10% present as mononuclear centers. The pheomelanin-αSyn-Fe conjugates are soluble and were characterized by NMR, LC-MS, EPR and ICP-OES. The present results show the possible mechanism of incorporation of αSyn into brain neuromelanin.

Keywords: neuromelanin; alpha-synuclein; DOPAL; DOPAC; melanin-protein conjugates; iron complexes

1. Introduction

The neuropathological hallmarks of Parkinson's Disease (PD) are the formation of Lewy bodies (LBs) and the progressive loss of dopaminergic neurons in *substantia nigra pars compacta* (SNpc) [1,2]. LBs appear as spherical filamentous protein inclusions formed by aggregated proteins (in particular α-synuclein, αSyn) and other cellular components that accumulate in parkinsonian patient neurons [3,4]. In addition, postmortem studies revealed the presence of Fe^{II} and Fe^{III} in LBs of PD patients [5–7]. Extensive evidence showed that in the

pathogenesis of PD a fundamental role is played by αSyn, an intrinsically disordered protein of 140 residues, localized at presynaptic terminals in close proximity to synaptic vesicles [8]. It is composed of three different domains: the N-terminal region, which encompasses residues 1–60, the highly hydrophobic self-aggregating sequence known as non-amyloid-component (NAC) which initiates fibrillation, constituted by residues 61–95, and the acidic C-terminal region, residues 96–140, which is essential for blocking rapid αSyn assembly (Scheme 1).

MDVFMKGLSKAKEGVVAAAEKTKQGVAEAAGKTKEG VLYVGSKTKEGVVHGVATVAEKTKEQVTNVGGAVVTG VTAVAQKTVEGAGSIAAATGFVKKDQLGKNEEGAPQEG ILEDMPVDPDNEAYEMPSEEGYQDYEPEA

Scheme 1. Amino acid sequence of αSyn.

The physiological role of αSyn has been related to membrane binding, synaptic vesicle recycling, dopamine (DA) and iron homeostasis [9,10] through multiple mechanisms, such as synthesis, storage, release, and DA reuptake. αSyn regulates the biosynthesis of DA by inhibiting the activity of tyrosine hydroxylase (TH), the key enzyme responsible for converting tyrosine to 3,4-dihydroxyphenylalanine in the DA synthesis pathway [11–13], which is also involved in biosynthesis of catecholamine-derived precursors of neuromelanin (NM) [14]. In addition, TH is an iron-dependent enzyme, so iron is essential in the synthesis and metabolism of DA [15,16]. αSyn itself in the C-terminal region contains a motif of negatively charged amino acids that potentially bind iron ions [17,18]. This effect is important as it has been shown that metal ion binding modulates the aggregation rate of αSyn [19]. In more general terms, both metal ions, such as iron and copper, and neurotransmitters, particularly DA, can influence αSyn structure and properties, both aggregation, membrane binding, and induction of toxic oxygen species [20,21].

It has been recently demonstrated by means of different techniques that αSyn is also present in NM of SN [22]. The NM pigment is a complex substance accumulated in specific neuronal organelles of different brain areas, and particularly in SN dopaminergic neurons [23], the main target of PD pathogenesis. αSyn could be part of the fibrillary proteins that form the NM core [11,24]. Several studies suggested that the interaction of NM with αSyn may be a mechanism for this pigment to modulate neuronal vulnerability, together with the removal of reactive or toxic *o*-quinones that would otherwise cause neurotoxicity [25,26]. DA can be also transformed within SN neurons without leading to the formation of NM, to the end of reducing its detrimental effects for the cell. Indeed, cytosolic DA can be metabolized in mitochondria by monoamine oxidase (MAO) to generate 3,4-dihydroxyphenyl acetaldehyde (DOPAL) [11]. In physiological conditions, DOPAL is detoxified by aldehyde dehydrogenase, which converts DOPAL to 3,4-dihydroxyphenylacetic acid (DOPAC), which undergoes further reduction to homovanillic acid (HVA) by catechol-*O*-methyltransferase, see Scheme 2 [11,27]. DOPAC and DOPAL, together with other DA metabolites, can be incorporated into NM [28]. It has to be noted that in the brain of PD patients the DOPAL:DA ratio was found to be higher than in the control subjects [29], suggesting that the mechanism of DA metabolism could be impaired in the disease [29]. Among the toxic effects of DOPAL, it has been shown that it binds to αSyn oligomers impairing synaptic vesicles functioning [30]. In addition, DOPAL binding to αSyn Lys residues promotes oxidation of all four Met residues, two in the N-terminal and two in the C-terminal region, an important post-translational αSyn modification in vivo [31]. Dopamination of αSyn by DA metabolites are not normally included among the post-translational modifications involved in PD pathogenesis [32], but it is quite certainly responsible for severe toxic effects on neuronal cells. Indeed, the high number of lysine residues and their easy accessibility in the natively unfolded αSyn make the protein a preferred target of reactions with a number of catabolic aldehydes, in addition to DOPAL, inducing toxic effects in the modified protein [33]. Also, DOPAC has been proposed to interact with αSyn, though non-covalently, preventing its fibrillation [34].

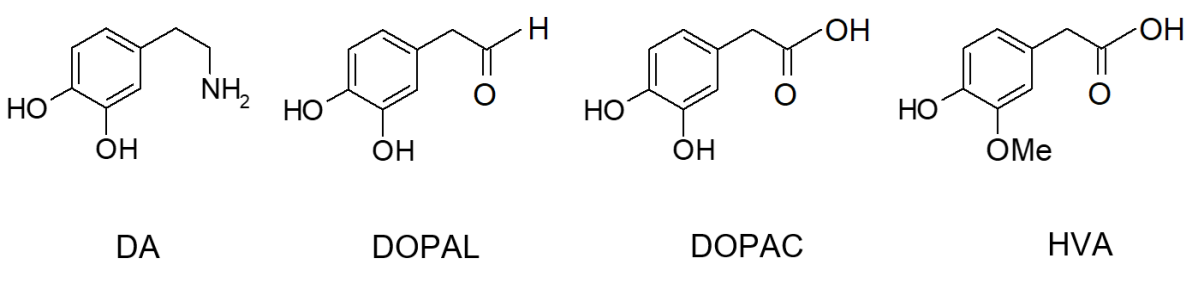

Scheme 2. Structure of DA and its metabolites.

Expanding upon our previous studies on synthetic analogues of NM based on DA-melanin-protein conjugates [35–37], in this study we aim at exploring the possible role of αSyn and DA metabolites in the formation of NM. To this end, we prepared several synthetic NMs by oxidative oligomerization of DA, DOPAL and DOPAC in the presence of αSyn, L-cysteine, and iron salts. The presence of cysteine makes the melanin-protein conjugates of pheomelanin type, resembling the inner core of human NM particles [38,39]. This work contributes to shedding light on the interaction between iron, DA metabolites and NM pathways whose interplay has consequences on neuronal vulnerability [40], fostering the development of new research on the interaction between neuronal proteins, metals and catecholamines in the formation of neuromelanin, and on its role in brain aging and PD pathology.

2. Materials and Methods

All reagents were purchased from Sigma–Aldrich (St. Louis, MO, USA). Recombinant human αSyn was produced using bacteria with reduced endotoxicity following the protocol previously used in our group [30]. All buffers and solutions were prepared with Milli-Q water. DOPAL was synthesized by rearrangement of epinephrine, following the method described by Robbins [41].

2.1. Preparation of Pheomelanin-αSyn-Iron(III) Conjugates

Protein-melanin conjugates were prepared by autoxidation of DA, DOPAL or DOPAC, in the presence of αSyn, following a procedure similar to that previously reported for the synthesis of melanin-albumin and melanin-lactoglobulin conjugates [36]. The samples were prepared in 0.05 M phosphate buffer (pH 7.4) by adding $Fe(NH_4)_2(SO_4)_2 \cdot 6H_2O$ to the solution of catecholamine, with a molar ratio of 0.05 of Fe with respect to DA/DOPAL/DOPAC, and further adding L-cysteine to the initial reaction mixture, with a 5:1 molar ratio of catecholamine/Cys, using the DA-DOPAL-DOPAC/αSyn ratio of 1:2 (*w*/*w*). The solutions were allowed to react in air at 37 °C for 4 days, protecting the reaction flask from light with an aluminum foil.

The solutions of conjugates thus obtained were dialyzed using tubing with a 10 kDa cutoff against milliQ water for 3 days, with a buffer-to-sample volume ratio of 50:1, and replacing the water six times, in order to eliminate unreacted DA/DOPAL/DOPAC and small quinone oligomers not bound to αSyn. The dialyzed conjugates were then freeze-dried to obtain a brown-black solid. The three types of melanin-αSyn-Fe conjugates obtained according to this procedure are labelled as DAPheoαSyn-Fe, DOPALPheoαSyn-Fe, and DOPACPheoαSyn-Fe.

2.2. NMR Quantification of Protein Content of the Conjugates

The protein content of the melanic conjugates was determined after complete acid hydrolysis and NMR quantification of the amino acids, according to the method of Ferrari et al. [35,36].

2.3. NMR Spectra of Pheomelanin-αSyn Conjugates

The ^{1}H-NMR spectra of the solutions were recorded on a Bruker AVANCE 400 spectrometer (Bruker BioSpin, Ettlingen, Germany) and acquired accumulating >2000 scans. Solutions for NMR were prepared by dissolving approximately 1 mg of conjugates in 1 mL of deuterium oxide under stirring for two days, keeping the solutions protected from light.

2.4. Analysis of the Protein Modification Sites in the Melanic Conjugates by Controlled Proteolysis and LC-MS Analysis

Proteolysis of αSyn conjugates was carried out without a denaturation process. About 1 mg of conjugate was dissolved in 20 mM ammonium bicarbonate buffer at pH 8.0 and digested with pepsin for 24 h at 37 °C after adjusting the pH to 1.3 with concentrated HCl. The amount of proteolytic enzyme was 2% *w*/*w* with respect to the protein. The digested peptides were separated and analyzed in automated LC-MS/MS mode using an LCQ ADV MAX ion trap mass spectrometer equipped with an ESI ion source and coupled with an automatic injector system Surveyor HPLC and controlled by Xcalibur software 1.3 (Thermo Finnigan, San Jose, CA, USA) according to the method of Ferrari et al. [36]. To identify the modified residues, the acquired MS/MS spectra were automatically searched against protein database for βLG using the SEQUEST® algorithm incorporated into Bioworks 3.1 software (Thermo Finnigan, San Jose, CA, USA).

2.5. Iron Analysis with ICP-OES

Weighted amounts of each sample were treated with 2 mL of Ultrapure 65% HNO_3 (Merck) refluxed for 10 min, evaporated to a small volume and diluted to 10 mL with ultrapure water. The clear solution thereby obtained was analyzed for the determination of the iron content. Appropriate blank solutions were treated in the same way and analyzed to probe the procedure. All the experimental measurements were performed in duplicate.

A Thermo Fischer Scientific ICP-OES iCAP 7400 was used for all the measurements, following operating conditions suggested by the manufacturer. The linearity range of intensity vs. iron concentration (0.1–10.0 mg/L) was obtained using standard solutions prepared from a 1 mg/mL stock solution; the limit of detection is 5 μg Fe/L, the limit of quantification is 15 μg Fe/L.

2.6. EPR Spectroscopy Measurements

EPR spectra were recorded at 10 K with an X band Bruker Elexsys E580 spectrometer (Bruker BioSpin, Ettlingen, Germany) equipped with a SHQ cavity and an Oxford ESR900 cryostat. The samples were prepared by dissolving 1.0–1.3 mg of each conjugate in 1.5 mL of MilliQ water upon stirring for 24 h at 28 °C. 250 μL of the dissolved samples were quickly mixed with 20% glycerol (for glass formation) just before being loaded in iron-free quartz EPR tubes (i.d. 3 mm). Nine scans were collected for each spectrum using the following spectrometer settings: modulation amplitude, 1 mT; conversion time, 82 ms; time constant, 41 ms; 2048 experimental points; wide scan range, 400 mT in order to simultaneously observe the iron(III) signal (g = 4.3) and the melanic radical signal (g = 2.0). Spectra were also collected in a narrower scan range in order to obtain a better resolved spectrum for the two signals.

The quantification of EPR-active iron(III) bound to conjugates, based on the g = 4.3 signal, was performed according to the protocol published by Chasteen and coworkers [42]. The calibration curve was constructed using Fe^{3+}-EDTA standard solutions prepared from a stock solution of known concentration of Fe^{3+} in hydrochloric acid (Iron Standard Solution in 0.1 M hydrochloric acid Prolabo).

3. Results and Discussion

3.1. Synthesis of the Conjugates

This study reports on the interaction of DA, DOPAL and DOPAC with αSyn to form covalent aggregates similar to those contained in human NM from SN. Our results show that the protein can be incorporated into the structure of the forming melanic polymer, with a covalent binding. The presence of cysteine makes the process of formation of the oligomeric conjugates complex to analyze. After Fe catalyzed oxidation of the catechol groups of the DA derivatives, the reaction of cysteine thiol with the resulting quinones is presumably the fastest event occurring in the mixture, with formation of the corresponding cysteinyl-DA derivatives [11,43]. These cysteinyl-catechols are electron rich and undergo iron-catalyzed oxidation to cysteinyl-quinones of DA, DOPAL and DOPAC, which can react with the nucleophilic groups present in αSyn, i.e., His50, the 15 Lys and the 4 Tyr residues, thereby forming the pheomelanin-protein core (Scheme 3). This core engulfs iron-oxo-hydroxo clusters linked through peripheral catechol groups of the melanin component. The cysteinyl-DA-quinone derivatives may undergo competitive internal cyclization to melanochromes [44], but this is not shown in the scheme because this possibility is precluded in the melanization pathways induced by DOPAL and DOPAC due to the lack of the primary amino group. In addition, in the case of DOPAL, the aldehyde groups can cross-link to the available unmodified Lys side chains of αSyn tightening the covalent linkage in the DOPALPheoαSyn-Fe conjugate. Also, the carboxylate group of DOPAC residues has the possibility to interact with free Lys side chains strengthening the melanin-protein interaction. Excess of catechol moieties of DA, DOPAL and DOPAC will add to the pheomelanic core of the conjugates to form an external eumelanic shell according to the process outlined previously [11].

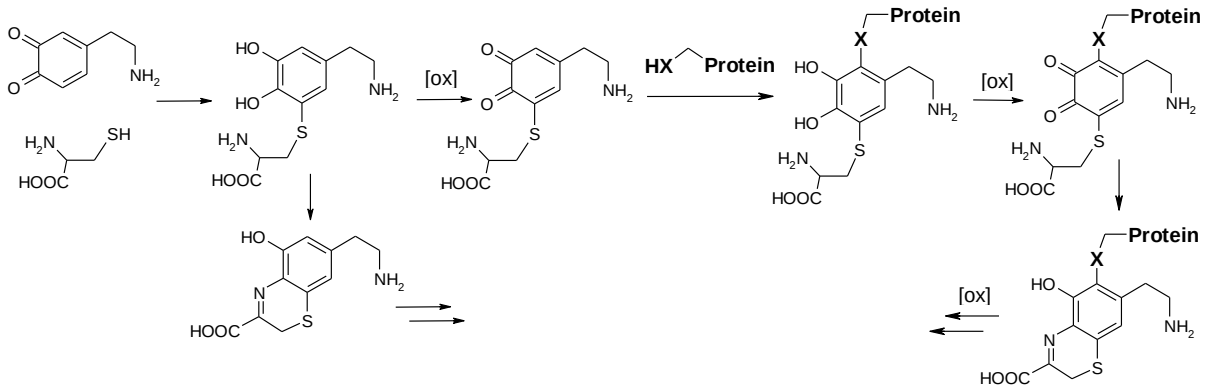

Scheme 3. Initial steps in the formation of the pheomelanin-protein core, shown here for the reaction of DA-quinone, cysteine and protein, that can be extended to the other dopamine metabolites (for simplicity only the 5-cysteinyl-DA isomer is shown).

3.2. Quantification of Protein and Iron Contents in the PheoαSyn-Conjugates

In the light of the previous considerations, we expect a tighter melanization process of αSyn in the conjugates formed from DOPAL and DOPAC than that from DA. This is confirmed by the percent protein fractions obtained from the hydrolysis of the DAPheoαSyn-Fe, DOPALPheoαSyn-Fe and DOPACPheoαSyn-Fe conjugates and the subsequent analysis through NMR spectroscopy (Table 1), which indicate a lower extent of melanization in the DAPheoαSyn-Fe derivative compared to the others. It is likely that in the case of DA-melanin, the ring closure of the amine group of the cysteinyl-DA quinone (Scheme 3), to form a melanochrome derivative [44], competes with the reaction of the protein lysines, resulting in lower extent of αSyn derivatization than for DOPAL and DOPAC.

The ICP-OES analysis confirmed the binding of iron ions to the conjugates (Table 1). The relative amount of Fe is in line with values found in NM from *substantia nigra* (about 10 μg/mg) [23].

Table 1. Percent protein content, iron amount, and percent EPR-detectable iron in PheoαSyn-conjugates (n = 2, RSD% ≤ 10%).

Sample	% Protein (*w*/*w*)	Iron (μg/mg)	% EPR Active Iron
DAPheoαSyn-Fe	58.0 ± 11.0	7.1	4
DOPALPheoαSyn-Fe	44.0 ± 12.0	5.2	9
DOPACPheoαSyn-Fe	45.0 ± 10.0	8.8	5

3.3. NMR Spectroscopy

To investigate the ^{1}H-NMR spectra of αSyn and synthetic PheoαSyn-Fe conjugates it is convenient to follow the proton signals of the aromatic amino acids (Phe and Tyr in αSyn) and the catechol moieties of the melanic components, while the aliphatic portion of the spectra contains broad and overlapping peaks that are difficult to decipher. In the aromatic region of the spectra, it is easier to see differences induced by the formation of melanin and its binding to the protein. The peaks in this region for αSyn are similar to those of phenylalanine and tyrosine in solution (Figure 1a), indicating that the aromatic side chains of the amino acids are free to rotate in solution. However, when αSyn is bound to the melanin, as in DAPheoαSyn-Fe, the aromatic groups are undergoing reduced mobility in solution, and this leads to some broadening of the signals (Figure 1b). The broadening is marked in the spectra of DOPALPheoαSyn-Fe and DOPACPheoαSyn-Fe derivatives (Figure 1c,d), probably due also to a larger size of the pheomelanin-αSyn conjugates because of the more extensive modification by melanic oligomers. It can be noted that the spectrum of DAPheoαSyn-Fe, where the extent of melanization is smaller (Table 1), shows signals of a small fraction of unmodified αSyn that is non-covalently bound and embedded in the melanic moiety.

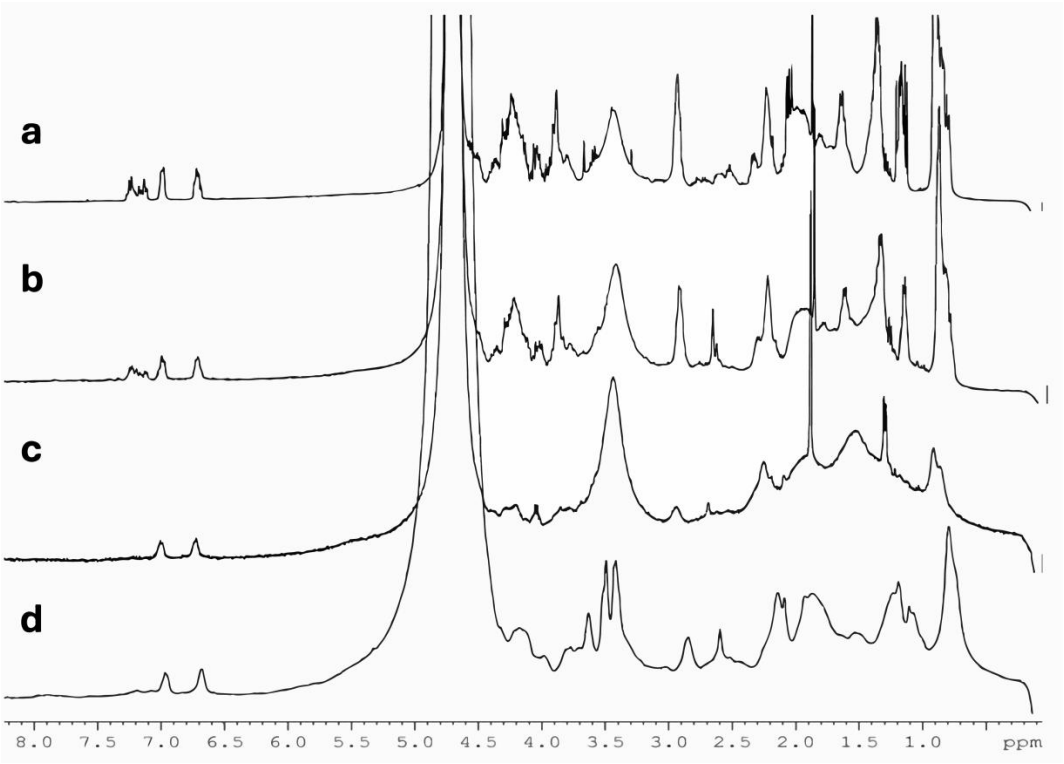

Figure 1. Proton NMR spectra in D_2O of (**a**) αSyn, (**b**) DAPheoαSyn-Fe, (**c**) DOPACPheoαSyn-Fe, (**d**) DOPALPheoαSyn-Fe.

3.4. Identification of Melanization Sites in the Protein Component of the Conjugates

In the initial phase of pheomelanin formation, as αSyn contains no cysteine, the possible binding sites of cysteinyl-DA-quinone, and DOPAL aldehyde group, are constituted by His50, the 15 lysines, and the four tyrosines contained in the αSyn sequence (Scheme 1). In order to clarify the role of the key residues in the αSyn melanization process, the melanin-αSyn conjugates were digested with pepsin and the peptide fragments were analyzed by LC-MS. The melanic portions covalently bound to the protein prevent the interaction with the digestive enzyme and thus the cleavage of the protein at the expected sites. Moreover, also the tandem MS fragmentation of the melanized peptides should be prevented. Therefore, the peptide fragments that are absent in the LC-MS analysis of the samples resulting from digestion are likely to contain the binding sites for DA quinones and are covalently linked to melanic oligomers, as successfully observed in past works on different protein-melanin conjugates [35,36]. In the digestion of the three different pheomelanin-αSyn conjugates the same fragments were unidentified, showing that the covalent melanization process occurs at the same sites for DA and its metabolites DOPAL and DOPAC. Several lysine residues were found to be involved in the interaction with quinones: K6, K10, K12, K58, K60 and, somewhat unexpectedly, no significant modification at histidine H50 (Table 2). Probably, the clustering of lysine residues in particular portions of the sequence make these residues more reactive towards DA-quinones. In addition, as there are no lysines, or other residues with nucleophilic side chains, in the missing C-terminal fragment (125–140), in this region the targets of reactive quinones are the three tyrosines Y125, Y133 and Y136. This is the first time that we unequivocally find modified Tyr residues in dopaminated protein. The analogy in fragmentation pattern confirms that also in the case of DAPheoαSyn-Fe the DA-melanin modification of αSyn occurs through the same mechanism as for the parent conjugates derived from DOPAL and DOPAC. Overall, these data confirm that the melanic oligomers are covalently bound to the protein and that αSyn is incorporated into the melanin.

Table 2. Fragments of αSyn that were not found upon digestion with pepsin of PheoαSyn-Fe conjugates.

PheoαSyn-Fe Conjugates
1–16 MDVFMKGLSKAKEGVV
54–69 TVAEKTKEQVTNVGGA
125–140 YEMPSEEGYQDYEPEA

3.5. Binding of Iron(III) to Pheomelanin Conjugates

The binding sites for iron are generally confined in the melanic portion of melanin-protein conjugates [35–37], though the C-terminal portion of αSyn rich of carboxylate residues (Scheme1) may make some minor contribution to iron binding. This is due to the fact that during the formation process of the conjugates, iron(III) ions are strongly bound to the catechol groups of the DA derivatives, keeping the Fe-oxo-hydroxo aggregates entrapped into the melanic oligomers. In any case, the coordination environment of the iron(III) centers is provided by oxygen donor atoms, similarly to brain NM [45]. Indeed, Mössbauer spectroscopy showed that the iron binding sites of brain NM contain oxygen donors and are similar to those of ferritin [46], but with metal centers assembled into clusters of smaller size linked by oxo-hydroxo bridges [24]. In addition, both in NM and in the melanin-protein conjugates, the iron(III) clusters are linked to the organic matrix through the catechol groups of melanin rather than amino acid residues of the protein, thus providing a different environment than ferritin.

3.6. Characterization of the Iron(III) Centers by EPR Spectroscopy

The EPR spectra of Pheo-αSyn-Fe conjugates recorded at 10 K exhibit two signals, one near g = 4.3, due to iron(III) and one at g = 2, due to the organic radical of the melanin (see Figure 2). The radical signal is clearly visible only for the DA conjugate and we assume that it is associated with the melanin portion which is not covalently bound to the protein. The iron(III) signal is broad and indicative of high-spin centers of rhombic symmetry, thus showing that pheomelanin-αSyn conjugates mimic adequately this feature of human NM, as observed in NMs purified from different human brain regions [23]. The intensity of the signal shows that the amount of EPR-detectable iron in Pheo-αSyn-Fe conjugates is much lower than the total amount of iron determined by ICP (Table 1). This result is in line with what we found previously for other melanin-protein-Fe conjugates [35–37] and with the fraction of <1% EPR active iron(III) generally found in brain NMs [23,47,48].

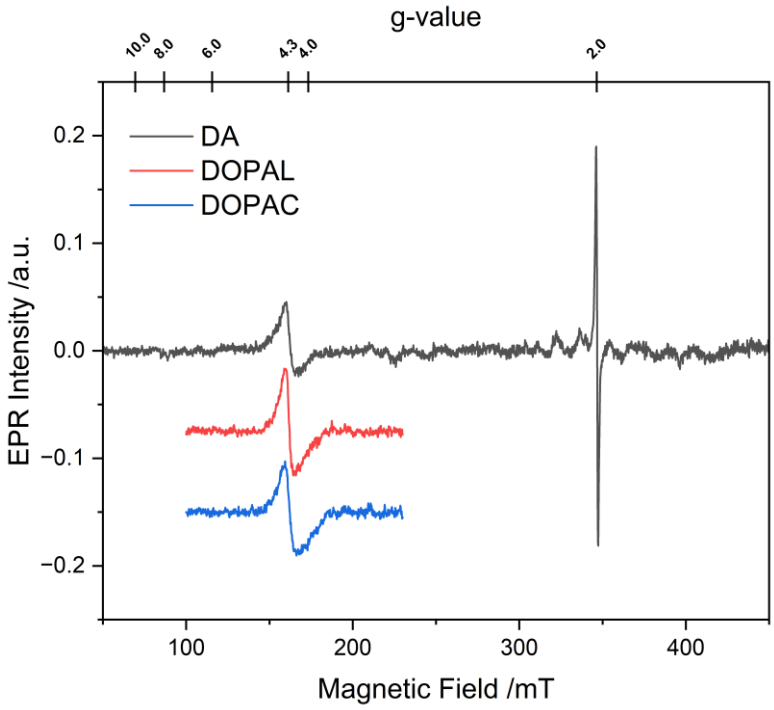

Figure 2. EPR spectra at 10 K of DAPheoαSyn-Fe (black); DOPALPheoαSyn-Fe (red); DOPALPheoαSyn-Fe (blue). The wide scan spectrum is shown for the DA conjugate to highlight the strong radical signal at g = 2, absent in the other samples.

4. Conclusions

The purpose of this study is to show that the interaction between oxidized DA derivatives, iron and αSyn can contribute to the formation of NM, as all of these components possibly play a crucial role in neurodegenerative processes, in particular of PD. Unlike previous studies on NM models which employed non-neuronal proteins to synthesize melanin-protein conjugates [35,36], here we demonstrated that synthetic NM analogues can be prepared starting from a neuronal protein such as αSyn that does not contain a Cys residue in the sequence, which is usually

considered as a key factor in the initial interaction between oxidized DA and protein [11,44,45]. An external cysteine can provide the more reactive cysteinyl-DA quinone derivative towards the protein lysines and tyrosines that in the case of αSyn constitutes the anchors for the growing (pheo)melanic chain (Scheme 3). The other functional groups present in the DA metabolites DOPAL (aldehyde) and DOPAC (carboxylate) can provide further covalent or ionic linkages strengthening the melanin-αSyn interaction. α-Syn is abundant in the brain and has been detected as one of the protein components of NM, and therefore shedding light into the mechanism of its inclusion within this substance is important. Like with iron, the incorporation of αSyn, likely in aggregated form, and the DA metabolites DOPAL and DOPAC into NM may be a mechanism to remove potentially toxic species from the cytosol. Further processing of the initial melanin-protein conjugates of NM and its inclusion into specialized organelles surrounded by a double membrane represent the further steps for completion of the protective mechanism [22,49].

Author Contributions

A.C., S.N., M.S., M.B. (Marco Bisaglia), G.F. and M.B. (Marco Bortolus) performed the experimental work. A.C., E.M., L.Z., F.A.Z., G.P., M.B. (Marco Bisaglia) and L.C. prepared and reviewed the manuscript. All authors have read and agreed to the published version of the manuscript.

Funding

The Authors E.M., M.S., S.N., A.C. and L.C. thank the University of Pavia for support. F.A.Z was supported by the Italian Ministry of University and Research (MUR)— "InvAt Project—Active and Healthy Aging (FOE 2022)". A.C and L.Z. thank the Pezzoli Foundation for Parkinson's disease (Milan, Italy) for financial support.

Data Availability Statement

Data supporting this study are included within the article.

Acknowledgments

M.S., S.N., L.C., and E.M. acknowledge MUR and the University of Pavia through the program "Dipartimenti di Eccellenza 2023–2027.

Conflicts of Interest

We confirm that neither the manuscript nor any parts of its content are currently under consideration or published in another journal.

References

1. Xu, L.; Nussinov, R.; Ma, B. Coupling of the non-amyloid-component (NAC) domain and the KTK(E/Q)GV repeats stabilize the α-synuclein fibrils. *Eur. J. Med. Chem.* **2016**, *121*, 841–850.
2. Morris, H.R.; Spillantini, M.G.; Sue, C.M.; et al. The pathogenesis of Parkinson's disease. *Lancet* **2024**, *403*, 293–304.
3. Bartels, T. A traffic jam leads to Lewy bodies. *Nat. Neurosci.* **2019**, *22*, 1039–1045.
4. Calabresi, P.; Di Lazzaro, G.; Marino, G.; et al. Advances in understanding the function of alpha-synuclein: Implications for Parkinson's disease. *Brain* **2023**, *146*, 3587–3597.
5. Lin, K.J.; Chen, S.D.; Lin, K.L.; et al. Iron brain menace: The involvement of ferroptosis in Parkinson disease. *Cells* **2022**, *11*, 3829.
6. Gaeta, A.; Hider, R.C. The crucial role of metal ions in neurodegeneration: The basis for a promising therapeutic strategy. *Br. J. Pharmacol*. **2005**, *146*, 1041–1059.
7. Brooks, J.; Everett, J.; Lermyte, F.; et al. Analysis of neuronal iron deposits in Parkinson's disease brain tissue by synchrotron x-ray spectromicroscopy. *J. Trace Elem. Med. Biol.* **2020**, *62*, 126555.
8. Goedert, M. Alpha-synuclein and neurodegenerative diseases. *Nat. Rev. Neurosci*. **2001**, *2*, 492–501.
9. Yavich, L.; Tanila, H.; Vepsäläinen, S.; et al. Role of alpha-synuclein in presynaptic dopamine recruitment. *J. Neurosci*. **2004**, *24*, 11165–11170.
10. Plotegher, N.; Greggio, E.; Bisaglia, M.; et al. Biophysical ground work as a hinge to unravel the biology of α-synuclein aggregation and toxicity. *Q. Rev. Biophys.* **2014**, *47*, 1–48.
11. Monzani, E.; Nicolis, S.; Dell'Acqua, S.; et al. Dopamine, oxidative stress and protein-quinone modifications in Parkinson's and other neurodegenerative diseases. *Angew. Chem. Int. Ed.*, **2019**, *58*, 6512–6527.
12. Lehrer, S.; Rheinstein, P.H. α-Synuclein enfolds tyrosine hydroxylase and dopamine ß-hydroxylase, potentially reducing dopamine and norepinephrine synthesis. *J. Proteins Proteom.* **2022**, *13*, 109–115.
13. Nagatsu, T.; Levitt, M.; Udenfriend, S.; Tyrosine hydroxylase. The initial step in norepinephrine biosynthesis. *J. Biol. Che.* **1964**, 239, 2910–2917.
14. Nagatsu, T.; Nakashima, A.; Watanabe, H.; et al. The role of tyrosine hydroxylase as a key player in neuromelanin synthesis and the association of neuromelanin with Parkinson's disease. *J. Neural Transm.* **2023**, *130*, 611–625.
15. Beard, J.; Erikson, K.M.; Jones, B.C. Neonatal iron deficiency results in irreversible changes in dopamine function in rats. *J. Nutr*. **2003**, *133*, 1174–1179.
16. Flydal, M.I.; Martinez, A. Phenylalanine hydroxylase: Function, structure, and regulation. *IUBMB Life* **2013**, *65*, 341–349.
17. Wu, K.P.; Kim, S.; Fela, D.A.; et al. Characterization of conformational and dynamic properties of natively unfolded human and mouse alpha-synuclein ensembles by NMR: Implication for aggregation. *J. Mol. Biol*. **2008**, *378*, 1104–1115.
18. Binolfi, A.; Rasia, R.M.; Bertoncini, C.W.; et al. Interaction of alpha-synuclein with divalent metal ions reveals key differences: A link between structure, binding specificity and fibrillation enhancement. *J. Am. Chem. Soc.* **2006**, *128*, 9893–9901.
19. Lorentzon, E.; Kumar, R.; Horvath, I.; et al. Differential effects of Cu^{2+} and Fe^{3+} ions on in vitro amyloid formation of biologically-relevant a-synuclein variants. *Biometals* **2020**, *33*, 97–106.
20. McDowall, J.S.; Brown, D.R. Alpha-synuclein: Relating metals to structure, function and inhibition. *Metallomics* **2016**, *8*, 385–397.
21. Sian-Hulsmann, J.; Riederer, P. The role of alpha-synuclein as ferrireductase in neurodegeneration associated with Parkinson's disease. *J. Neural Transm.* **2020**, *127*, 749–754.
22. Zucca, F.A.; Vanna, R.; Cupaioli, F.A.; et al. Neuromelanin organelles are specialized autolysosomes that accumulate undegraded proteins and lipids in aging human brain and are likely involved in Parkinson's disease. *NPJ Park. Dis.* **2018**, *4*, 17.
23. Zecca, L.; Bellei, C.; Costi, P.; et al. New melanic pigments in the human brain that accumulate in aging and block environmental toxic metals. *Proc. Natl. Acad. Sci. USA* **2008**, *105*, 17567–17572.
24. Zucca, F.A.; Segura-Aguilar, J.; Ferrari, E.; et al. Interactions of iron, dopamine and neuromelanin pathways in brain aging and Parkinson's disease. *Prog. Neurobiol.* **2017**, *155*, 96–119.
25. Xu, S.; Chan, P. Interaction between neuromelanin and alpha-synuclein in Parkinson's disease. *Biomolecules* **2015**, *5*, 1122–1142.
26. Xuan, Q.; Xu, S.L.; Lu, D.H.; et al. Increased expression of α-synuclein in aged human brain associated with neuromelanin accumulation. *J. Neural Transm.* **2011**, *118*, 1575–1583.
27. Nagatsu, T.; Nakashima, A.; Wakamatsu, K. Neuromelanin in Parkinson's disease: Tyrosine hydroxylase and tyrosinase. *Int. J. Mol. Sci*. **2022**, *23*, 4176.
28. Wakamatsu, K.; Tanaka, H.; Tabuchi, K.; et al. Reduction of the nitro group to amine by hydroiodic acid to synthesize o-aminophenol derivatives as putative degradative markers of neuromelanin. *Molecules* **2014**, *19*, 8039–8050.

29. Jinsmaa, Y.; Cooney, A.; Sullivan, P.; et al. The serotonin aldehyde, 5-HIAL, oligomerizes alpha-synuclein. *Neurosci. Lett*. **2015**, *590*, 134–137.
30. Plotegher, N.; Berti, G.; Ferrari, E.; et al. DOPAL derived alpha-synuclein oligomers impair synaptic vesicles physiological function. *Sci. Rep.* **2017**, *7*, 40699.
31. Carmo-Gonçalves, P.; do Nascimento, L.A.; Cortines, J.R.; et al. Exploring the role of methionine residues on the oligomerization and neurotoxic properties of DOPAL-modified α-synuclein. *Biochem. Biophys. Res. Commun*. **2018**, *505*, 295–301.
32. He, S.; Wang, F.; Yung, K.K.L.; et al. Effects of α-synuclein-associated post-translational modifications in Parkinson's disease. *ACS Chem. Neurosci.* **2021**, *12*, 1061–1071.
33. Plotegher, N.; Bubacco, L. Lysines, Achilles' heel in alpha-synuclein conversion to a deadly neuronal endotoxin. *Aging Res. Rev*. **2016**, *26*, 62–71.
34. Zhou, W.; Gallagher, A.; Hong, D.-P.; et al. At low concentrations, 3,4-dihydroxyphenylacetic acid (DOPAC) binds non-covalently to alpha-synuclein and prevents its fibrillation**.** *J. Mol. Biol*. **2009**, *388*, 597–610.
35. Ferrari, E.; Engelen, M.; Monzani, E.; et al. Synthesis and structural characterization of soluble neuromelanin analogs provides important clues to its biosynthesis. *J. Biol. Inorg. Chem*. **2013**, *18*, 81–93.
36. Ferrari, E.; Capucciati, A.; Prada, I.; et al. Synthesis, structure characterization, and evaluation in microglia cultures of neuromelanin analogues suitable for modeling Parkinson's disease. *ACS Chem. Neurosci*. **2017**, *8*, 501–512.
37. Capucciati, A.; Monzani, E.; Sturini, M.; et al. Water-soluble melanin–protein–Fe/Cu conjugates derived from norepinephrine as reliable models for neuromelanin of human brain *locus coeruleus. Angew. Chem. Int. Ed*. **2022**, *61*, e202204787.
38. Ito, S. Encapsulation of a reactive core in neuromelanin. *Proc. Natl. Acad. Sci. USA* **2006**, *103*, 14647–14648.
39. Bush, W.D.; Garguilo, J.; Zucca, F.A.; et al. The surface oxidation potential of human neuromelanin reveals a spherical architecture with a pheomelanin core and a eumelanin surface. *Proc. Natl. Acad. Sci. USA* **2006**, *103*, 14785–14789.
40. Wise, R.M.; Wagener, A.; Fietzek, U.M.; et al. Interactions of dopamine, iron, and alpha-synuclein linked to dopaminergic neuron vulnerability in Parkinson's disease and neurodegeneration with brain iron accumulation disorders. *Neurobiol. Dis*. **2022**, *175*, 105920.
41. Robbins, J.H. Preparation and properties of *p*-hydroxyphenylacetaldehyde and *3*-methoxy-4-hydroxyphenylacetaldehyde. *Arch. Biochem. Biophys.* **1966**, *114*, 576–584.
42. Bou-Abdallah, F.; Chasteen, N.D. Spin concentration measurements of high-spin (g' = 4.3) rhombic iron(III) ions in biological samples: Theory and application. *J. Biol. Inorg. Chem*. **2008**, *13*, 15–24.
43. Ito, S.; Sugumaran, M.; Wakamatsu, K. Chemical reactivities of ortho-quinones produced in living organisms: Fate of quinonoids produced by tyrosinase and phenoloxidase action on phenols and catechols. *Int. J. Mol. Sci*. **2020**, *21*, 6080.
44. Wakamatsu, K.; Nakao, K.; Tanaka, H.; et al. The oxidative pathway to dopamine–protein conjugates and their pro-oxidant activities: Implications for the neurodegeneration of Parkinson's disease. *Int. J. Mol. Sci.* **2019**, *20*, 2575.
45. Zucca, F.A.; Capucciati, A.; Bellei, C.; et al. Neuromelanins in brain aging and Parkinson's disease: Synthesis, structure, neuroinflammatory, and neurodegenerative role. *IUBMB Life* **2023**, *75*, 55–65. https://doi.org/10.1002/iub.2654.
46. Arosio, P.; Elia, L.; Poli, M. Ferritin, cellular iron storage and regulation. *IUBMB Life* **2017**, *69*, 414–422.
47. Zecca, L.; Shima, T.; Stroppolo, A.; et al. Interaction of neuromelanin and iron in substantia nigra and other areas of human brain. *Neuroscience* **1996**, *73*, 407–415.
48. Zecca, L.; Stroppolo, A.; Gatti, A.; et al. The role of iron and copper molecules in the neuronal vulnerability of locus coeruleus and substantia nigra during aging. *Proc. Natl. Acad. Sci. USA* **2004**, *101*, 9843–9848.
49. Capucciati, A.; Zucca, F.A.; Monzani, E.; et al. Interaction of neuromelanin with xenobiotics and consequences for neurodegeneration; promising experimental models. *Antioxidants* **2021**, *10*, 824.